

# New Insights into the Molecular Mechanism of Multiple Synostoses Syndrome (SYNS): Mutation Within the GDF5 Knuckle Epitope Causes Noggin-Resistance

Gerburg K. Schwaerzer,<sup>1</sup> Christian Hiepen,<sup>1</sup> Heinrich Schrewe,<sup>2</sup> Joachim Nickel,<sup>3</sup> Frank Ploeger,<sup>4</sup> Walter Sebald,<sup>5</sup> Thomas Mueller,<sup>6</sup> and Petra Knaus<sup>1</sup>

<sup>1</sup>Institute for Chemistry and Biochemistry, Free University Berlin, Berlin, Germany

<sup>2</sup>Institute for Medical Genetics—CBF, Charité-University Medicine Berlin, Berlin, Germany; and Max Planck Institute for Molecular Genetics, Berlin, Germany

<sup>3</sup>Institute for Tissue Engineering and regenerative Medicine, Universitaetsklinikum Wuerzburg, Wuerzburg, Germany

<sup>4</sup>Biopharm GmbH, Heidelberg, Germany

<sup>5</sup>Theodor-Boveri-Institute for Biosciences, University Wuerzburg, Wuerzburg, Germany

<sup>6</sup>Institute for Plant Physiology and Biophysics, University Wuerzburg, Wuerzburg, Germany

## ABSTRACT

Growth and differentiation factor 5 (GDF5), a member of the bone morphogenetic protein (BMP) family, is essential for cartilage, bone, and joint formation. Antagonists such as noggin counteract BMP signaling by covering the ligand's BMP type I (BMPRI) and type II (BMPRII, ActRII, ActRIIB) interaction sites. The mutation GDF5-S94N is located within the BMPRII interaction site, the so-called knuckle epitope, and was identified in patients suffering from multiple synostoses syndrome (SYNS). SYNS is characterized by progressive symphalangism, carpal/tarsal fusions, deafness and mild facial dysmorphism. Here we present a novel molecular mechanism of a GDF5 mutation affecting chondrogenesis and osteogenesis. GDF5-S94N exhibits impaired binding to BMPRII causing alleviated Smad and non-Smad signaling and reduced chondrogenic differentiation of ATDC5 cells. Surprisingly, chondrogenesis in mouse micromass cultures was strongly enhanced by GDF5-S94N. By using quantitative techniques (SPR, reporter gene assay, ALP assay, qPCR), we uncovered that this gain of function is caused by strongly reduced affinity of GDF5-S94N to the BMP/GDF antagonist noggin and the consequential lack of noggin inhibition. Thus, since noggin is upregulated during chondrogenic differentiation, GDF5-S94N exceeds the GDF5 action, which results in the phenotypic outcome of SYNS. The detailed molecular characterization of GDF5-S94N as a noggin-resistant growth factor illustrates the potential of GDF5 mutants in applications with defined therapeutic needs. © 2012 American Society for Bone and Mineral Research.

**KEY WORDS:** GDF5; BMPRII; KNUCKLE EPILOPE; NOGGIN; MULTIPLE SYNOSTOSES SYNDROME

## Introduction

Bone morphogenetic proteins (BMPs) and growth and differentiation factors (GDFs) are crucial regulators of bone and cartilage development and homeostasis. Many bone and cartilage diseases in humans can be traced back to mutations in this BMP ligand family, their receptors, and/or their extracellular antagonists.<sup>(1–6)</sup> GDF5 itself is a key regulator of chondrogenic differentiation and joint formation controlling the number and length of limb bones.<sup>(7)</sup> At early stages of chondrogenesis GDF5 is secreted in condensing mesenchyme of the limb to stimulate

recruitment and differentiation of chondrogenic precursor cells. Later it is expressed at sites of subsequent joint formation (reviewed before).<sup>(8)</sup> GDF5 binds a set of BMP type I (BMPRIA/B) and type II receptors (BMP receptor type II, BMPRII, and Activin receptor type II/ IIB, ActRII/ActRIIB), assembled either as preformed complex (PFC) or in the BMP-induced signaling complex (BISC).<sup>(9,10)</sup> Upon ligand binding to PFCs, the constitutive active BMPRII phosphorylates and thereby activates BMPRIA/B, which in turn phosphorylates receptor regulated Smads (R-Smads, namely, Smad 1/5/8). Activated R-Smads form heteromeric complexes with Smad 4, translocate into the

Received in original form May 27, 2011; revised form August 10, 2011; accepted August 29, 2011. Published online October 4, 2011.

Address correspondence to: Petra Knaus, PhD, Institute for Chemistry and Biochemistry, Free University Berlin, Thielallee 63, 14195 Berlin, Germany.

E-mail: knaus@chemie.fu-berlin.de

Additional Supporting Information may be found in the online version of this article.

Journal of Bone and Mineral Research, Vol. 27, No. 2, February 2012, pp 429–442

DOI: 10.1002/jbmr.532

© 2012 American Society for Bone and Mineral Research

nucleus to bind to specific DNA sites where they induce target gene transcription. As a second binding mode, BMP family ligands such as GDF5 or BMP2 can bind the high-affinity type I receptor first and recruit the low-affinity type II receptor into a BISC, which triggers non-Smad signaling, for example, via the p38 mitogen activated kinase (MAPK) pathway.<sup>(11,12)</sup> Both signaling pathways modulate target gene expression and are involved in the regulation of chondrogenesis.<sup>(13,14)</sup> Proper chondrogenesis is required for the later onset of bone formation via endochondral ossification (reviewed earlier).<sup>(15)</sup> To gradually finetune BMP signaling during endochondral ossification natural antagonists such as noggin are expressed. Noggin interacts with BMPs to inhibit their receptor interaction.<sup>(16,17)</sup>

Several mutations within GDF5 are identified causing chondrodysplasia,<sup>(18–20)</sup> brachydactyly,<sup>(21–23)</sup> symphalangism (SYM),<sup>(22,24,25)</sup> or the multiple synostoses syndrome (SYNS).<sup>(26–28)</sup>

The point mutation GDF5-S94N (or S475N when the proprotein numbering is considered) is a gain of function mutation resulting in SYNS. Patients suffer from carpal/tarsal coalition, proximal symphalangism, humeroradial synostosis, as well as progressive conductive deafness.<sup>(26)</sup> The molecular mechanisms leading to this progressive chondrogenic and osteogenic phenotype are unknown so far. The mutation S94N is located within the so-called knuckle epitope, the interaction site of GDF5 with its BMP type II receptors. Serine 94 is one out of the five residues identified in the related BMP2 ligand as important determinants for BMP type II receptor binding.<sup>(29)</sup> It is located in the center of the hydrophobic interface between BMPs and BMP receptor type II and forms intermolecular H-bonds with ActRII or ActRIIB.<sup>(30,31)</sup> We used Surface Plasmon Resonance measurements (SPR) in combination with cellular assays to gain deeper insights into the molecular mechanisms and signaling potency of GDF5-S94N compared with wild-type GDF5 and the variant GDF5-L60P, which has contrary in vitro binding properties to the type I and type II BMP receptors compared with GDF5-S94N. GDF5-L60P (or L441P when the proprotein numbering is considered) was previously identified as a loss-of-function mutation located in close proximity to the wrist epitope, important for interaction with the type I receptors BMPRIA or IB.<sup>(22)</sup> Interestingly, in contrast to GDF5-S94N, the mutant GDF5-L60P is described to cause brachydactyly type A2 (BDA2), which is characterized by reduced chondrogenesis and attenuated osteogenesis leading to shortened fingers because hypoplasia of phalanges or missing phalanges.<sup>(22)</sup> The same phenotype was also identified in patients with a mutation in BMPRIIB.<sup>(2)</sup>

In the study presented here we treated mesenchymal C2C12 cells, prechondroblastic ATDC5 cells, and mouse micromass cultures with recombinant GDF5, GDF5-S94N, and GDF5-L60P. Hereby we aimed to uncover the molecular mechanisms responsible for the phenotypes of SYNS and BDA2. We show that the SYNS mutation GDF5-S94N, located within the type II receptor binding epitope, exhibited a reduced binding affinity to BMPRII but was nevertheless able to trigger strongly enhanced BMP/GDF signaling and chondrogenesis because a lack of noggin inhibition. Furthermore, we uncovered that the BDA2 mutant GDF5-L60P failed to induce Smad signaling and p38 MAPK activation, which impairs chondrogenesis.

## Material and Methods

### Antibodies

Antibodies were obtained from the following sources: antiphospho p38 (1:1000) from Promega (Madison, WI, USA), anti- $\beta$  actin (1:5000) from Sigma-Aldrich (St. Louis, MO, USA), antiphospho-Smad 1/5/8 (1:1000), anti-Lamin A/C (1:1000), and anti-GAPDH (1:1000) from Cell Signaling (Danvers, MA, USA). For immunofluorescence staining we used anti-Smad1 (1:500) from Cell Signaling and anti-myosin (1:500) from Sigma-Aldrich.

### Cell culture

C2C12 cells (American Type Culture Collection [ATCC], Rockville, MD, USA) were cultivated in Dulbecco's modified eagle medium (DMEM) supplemented with 10% fetal bovine serum (FBS), 100 U/mL penicillin, and 100 mg/mL streptomycin. ATDC5 cells (Riken Cell Bank, Japan) were cultivated in DMEM/Ham's F12 supplemented with 5% FBS plus 100 U/mL penicillin and 100 mg/mL streptomycin.

### Luciferase-based reporter gene assay

Cells were seeded using a 24-well plate at  $1 \times 10^4$  cells per well. After 24 hours, cells were transfected with pBRE-Luc<sup>(32)</sup> or pMyg-Luc (myogenin promoter driving firefly luciferase) and pRLTK (Promega) using Lipofectamine 2000 (Invitrogen, Carlsbad, CA, USA). Cells were starved for 5 hours and stimulated with ligand in the presence of 0.5% FBS for 16 hours (BRE-Luc) or for 5 days (Myg-Luc). Luciferase activity was measured using the Dual Glow luciferase reporter assay system (Promega) and a Mithras LB 940 luminometer (Berthold Detection Systems, Pforzeim, Germany).

### Phospho-p38 and phospho-Smad assays

C2C12 cells were seeded in a six-well plate at  $1 \times 10^5$  cells per well. After 24 hours, cells were starved for 3 hours and incubated in the absence or presence of 10 nM ligand for 30 minutes or the indicated times. Cells were washed with PBS, lysed in SDS-sample buffer, and applied on 10% PAA gels for Western blotting analysis.

### Cell fractionation

Cells were seeded in a six-well plate at  $4 \times 10^5$  cells per well, starved for 3 hours and stimulated with 10 nM ligand for the indicated times. Cytoplasmic and nuclear proteins were isolated using ProteoJet Extraction Kit (Fermentas, Hanover, MD, USA) according to manufacturer's instruction.

### Immunofluorescence

Cells ( $3 \times 10^4$ ) were plated on glass coverslips placed in 24-well plates. After 24 hours cells were stimulated with 10 nM ligand in DMEM containing 0.5% FBS for the indicated times. Immunofluorescence staining and microscopy were performed as described previously.<sup>(33)</sup>

### Alkaline phosphatase (ALP) assay

Cells were seeded in 96-well plates at  $1 \times 10^4$  per well and incubated with ligand (DMEM, 2% FBS) for 72 hours in the

absence or presence of increasing concentrations of noggin (R&D Systems, Minneapolis, MN, USA). Cells were washed with phosphate-buffered saline (PBS) and lysed in lysis buffer (100 mM glycine/Na<sup>+</sup> pH 9.6, 1 mM MgCl<sub>2</sub>, 1 mM ZnCl<sub>2</sub>, 1% NP-40). Absorption at 405 nm was measured using an ELISA-plate reader (Tecan, Männedorf, Switzerland).

### Quantitative PCR (qPCR)

Total RNA was extracted using NucleoSpin RNA extraction kit (Macherey and Nagel, Düren, Germany) according to manufacturer's instructions. cDNA was obtained by reverse transcription of total RNA. Quantification of genes was assessed by qPCR using the StepOne Plus and SYBR Green PCR Master Mix (Applied Biosystems, Bedford, MA, USA). The transcript expression level was normalized to HPRT.

### Surface plasmon resonance (SPR) measurements

SPR were carried out using a Biacore 2000 system.<sup>(10,22)</sup> In brief, 200 to 500 resonance units (RU) of either N-biotinylated receptor or noggin proteins were immobilized to streptavidin coated CM5 chips. Interaction sensorgrams were recorded at a flow rate of 10 μL/min at 25 °C. Association and dissociation times were set to 5 minutes. After each cycle the chips were regenerated with 4 M MgCl<sub>2</sub> and additionally with a regeneration solution containing 1 mM acetic acid, 1 M NaCl, and 6 M Urea for 2 minutes. HB500 buffer (10 mM HEPES pH 7.4, 500 mM NaCl, 3.4 mM EDTA, 0.005% surfactant P20) was used as running buffer for all experiments.

### Micromass cultures

Primary limb mesenchymal cultures were established from E11.5 CD1 mouse embryos (mouse facility at Max Planck Institute for Molecular Genetics) after Karamboulas et al.<sup>(34)</sup> with some

modifications. Briefly, limb buds were dissected and ectoderm removed after digestion in dispase/collagenase solution (3 mg/mL Dispase/Collagenase [Roche, Indianapolis, IN, USA] in Hank's Balanced Salt Solution [HBSS]). Cells were isolated from limb buds after digestion with collagenase/trypsin (0.1% collagenase type Ia [Sigma-Aldrich], 0.1% trypsin [Invitrogen], 5% FBS in PBS), filtered through a 40 μm-cell strainer (BD Falcon, Bedford, MA, USA), resuspended in culture medium (DMEM/F12 [Invitrogen], 10% FBS) at a density of 2 × 10<sup>7</sup> cells/mL, and seeded in 10 μL drops (2 × 10<sup>5</sup> cells). After 2 hours, cells were stimulated with recombinant GDF5, GDF5-L60P, GDF5-S94N (proteins supplied by Biopharm GmbH), and BMP2 (W. Sebald, Wuerzburg, Germany) in the absence or presence of noggin (R&D Systems). Medium was changed every 48 hours. After 6 days, micromass cultures were fixed and stained with 1% Alcian Blue stain (Sigma-Aldrich) pH 1.0 overnight. Staining was quantified using BIO-1D (Vilber-Lourmat, Marne-la-Vallée, France). Three replicas for each condition were performed in parallel.

### Statistical analysis

Statistical analysis was performed using a two-tailed Student's *t* test.

## Results

### Mutation within GDF5 affects binding properties to BMP receptors

In SYNS patients, the serine residue at position 94 of mature GDF5 is exchanged by asparagine (GDF5-S94N) because of a point mutation.<sup>(26)</sup> This serine residue is highly conserved amongst the GDF/BMP family (Fig. 1A) and located in the β-sheet β6 of the knuckle epitope (Fig. 1B). The knuckle epitope consists of β-sheets β2–β4 of finger 1 and β6 and β7 of finger 2 forming a

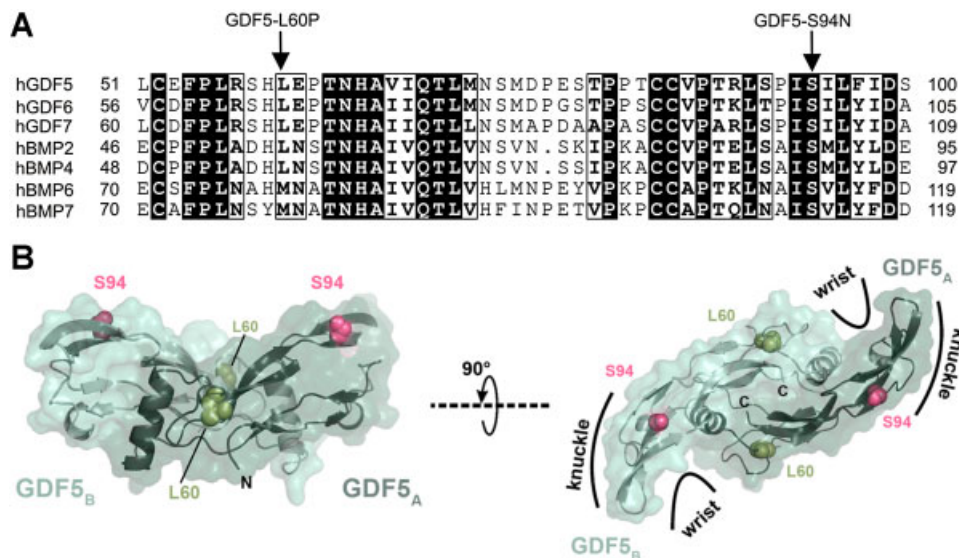


**Fig. 1.** Localization of the GDF5-L60P and GDF5-S94N mutation in GDF5. (A) Sequence alignments of different mature human GDF and BMP ligands. Arrows indicate the mutation sites for GDF5-L60P and GDF5-S94N. (B) Ribbon presentation of the GDF5<sub>A,B</sub> dimer (surfaces shown in dark and light green). The location of exchanged amino acids in GDF5-S94N (pink) and GDF5-L60P (green) are indicated. The ribbon model (right) is rotated around the x axis by 90° and depicts the wrist epitopes (type I receptor binding site) and the knuckle epitopes (type II receptor binding site) of GDF5.

convex surface (Fig. 1B). It interacts with the concave surface of BMP type II receptors, which is formed by three pairs of antiparallel  $\beta$ -sheets.<sup>(30,35,36)</sup>

We compared the signaling potency of GDF5-S94N with GDF5 and the previously published GDF5-L60P mutant causing BDA2. The latter point mutation is located next to the wrist epitope (Fig. 1B).<sup>(22,35,37)</sup> We first analyzed ligand binding to the BMP type I receptors BMPRIA and IB as well as to BMPRII by SPR (Table 1) using immobilized receptors. According to the phenotype of SYNS1, which indicates a gain of function mutation we expected an elevated binding affinity of GDF5-S94N for BMPRII. However, the variant GDF5-S94N binds BMPRII ( $K_D \sim 180$  nM) with about fivefold lower affinity compared with GDF5 ( $K_D \sim 35$ – $40$  nM), whereas the affinity of GDF5-S94N for BMPRIA ( $K_D \sim 20$  nM) and BMPRIB ( $K_D \sim 1$  nM) was unaffected (Table 1). The variant GDF5-L60P characterized as a loss of function mutation showed no detectable binding affinity to BMPRIA and strongly reduced binding to BMPRIB ( $K_D \sim 42,3$  nM)<sup>(35)</sup> (Table 1). Hence, GDF5-S94N and GDF5-L60P exhibit contrary in vitro binding properties to BMPRIA/IB and BMPRII receptors.

### The S94N mutation within the knuckle epitope of GDF5 inhibits Smad signaling

GDF5 and BMP2 are homologous on the one hand, but display distinct binding preferences for type I receptors. GDF5 binds more strongly to BMPRIB ( $K_D \sim 1$  nM) compared with BMPRIA ( $K_D \sim 20$  nM), whereas BMP2 binds BMPRIA ( $K_D \sim 1$  nM) and BMPRIB ( $K_D \sim 2$ – $3$  nM) with almost similar affinities (Table 1).<sup>(37,38)</sup> Because GDF5 regulates the condensation of mesenchymal cells in limbs as well as chondrogenic differentiation, we used mesenchymal C2C12 cells, prechondroblastic ATDC5 and micromass cells generated from mouse limb buds. Because C2C12 cells are well characterized for BMP2 signaling, we included BMP2 as a positive-control.

At the cell surface numerous combinations of BMP receptor oligomers exist, even in the absence of ligands.<sup>(39)</sup> Similar to BMP2, GDF5 binds preformed BMPRIA/IB:BMPRII and induces Smad-dependent signaling.<sup>(9,12,40)</sup> Therefore, we examined both GDF5-S94N and GDF5-L60P for their ability to induce Smad 1/5/8 phosphorylation, Smad translocation and Smad-dependent target gene transcription. We found that the GDF5-S94N mutant induced Smad 1/5/8 phosphorylation with about fivefold lower efficiency than GDF5 and BMP2 (Fig. 2A). The GDF5-L60P mutant was ineffective in inducing Smad phosphorylation (Fig. 2A).

**Table 1.** Binding Affinities of GDF5 Mutants to Immobilized Receptors (SPR Measurement)

Ligand	$K_D$ (nM)			Ref.
	BMPRIA	BMPRIB	BMPRII	
BMP2	0.8	2.4	45	(37,62)
GDF5	19	1.3	36	
GDF5-L60P	n.b.	42.3	31.9	(22,35)
GDF5-S94N	19.5	1.2	183.7	

Mean values from two experiments using at least six different analyte concentrations.

Similar results were obtained by analyzing Smad nuclear translocation (Fig. 2B). To support our data we further examined the immediate effects of ligand stimulation using cell fractionation. Our experiments revealed a delayed phospho-Smad nuclear translocation in GDF5-S94N and GDF5-L60P treated cells in comparison to GDF5 (Fig. 2C). In detail, stimulation with GDF5-S94N for 30 minutes resulted in strong Smad 1/5/8 phosphorylation in the cytoplasm, but compared with GDF5 less phospho-Smad accumulated in the nucleus (Fig. 2C, upper panel, compare lanes 1, 3, 5, and 6, 8, 10). Upon 45 minutes or 60 minutes stimulation with the GDF5-S94N mutant the amount of nuclear phospho-Smad 1/5/8 adjusted more to the nuclear phospho-Smad 1/5/8 levels induced by GDF5 (Fig. 2C, lower panels, compare lanes 6, 8, and 10). In contrast to that, GDF5-L60P did not stimulate Smad 1/5/8 nuclear translocation after 30 and 45 minutes. Only after 60 minutes of treatment with GDF5-L60P we could detect nuclear Smads, which might be caused by indirect mechanisms (Fig. 2C, compare lanes 6, 8, and 9). We next investigated the effects of these GDF5 mutants on Smad-dependent target gene expression using BMP responsive element (BRE) gene construct driving a luciferase reporter (BRE-Luc).<sup>(32)</sup> The GDF5-S94N mutant displayed strongly reduced reporter gene activity compared with GDF5, whereas the GDF5-L60P mutant did not show any ability to induce the BRE reporter (Fig. 2D).

Hence, the lower BMPRII affinity of the SYNS associated GDF5-S94N mutant results in decreased Smad phosphorylation, delayed Smad nuclear translocation and weaker Smad-dependent transcriptional activity. GDF5-L60P is deficient in immediate Smad activation and nuclear translocation as well as reporter gene activation caused by severely impaired type I receptor binding.

### GDF5-S94N shows a delay in MAPK activation

GDF5 and BMP2 bind type I and type II receptor subsequently and activate the p38 MAPK pathway.<sup>(10,11,13)</sup> To test, whether GDF5-S94N signals via BISCs and activates p38, we investigated p38 phosphorylation at different time points. GDF5 and BMP2, as well as GDF5-S94N, induced p38 phosphorylation (Fig. 3), however, with distinct signaling dynamics. In detail, BMP2 and GDF5 induced p38 phosphorylation after 30 minutes and the signal sustained until 60 minutes. The GDF-S94N variant displayed no immediate signaling (30 minutes), but a delayed p38 phosphorylation culminating at 45 minutes (Fig. 3). In contrast, GDF5-L60P completely failed to induce p38 phosphorylation. Thus, proper binding to the type I receptors is crucial for phosphorylation of p38 MAPK. As our data suggest, an efficient interaction of the ligand with BMPRII might be necessary for rapid signal propagation.

The GDF5 variant S94N is less potent in myoblast/osteoblast conversion of C2C12 and chondrogenic maturation of ATDC5 cells

The BMP/GDF dependent activation of both the Smad- and non-Smad pathways is necessary to potently induce osteogenic differentiation of C2C12 cells.<sup>(41,42)</sup> If C2C12 cells are not directed

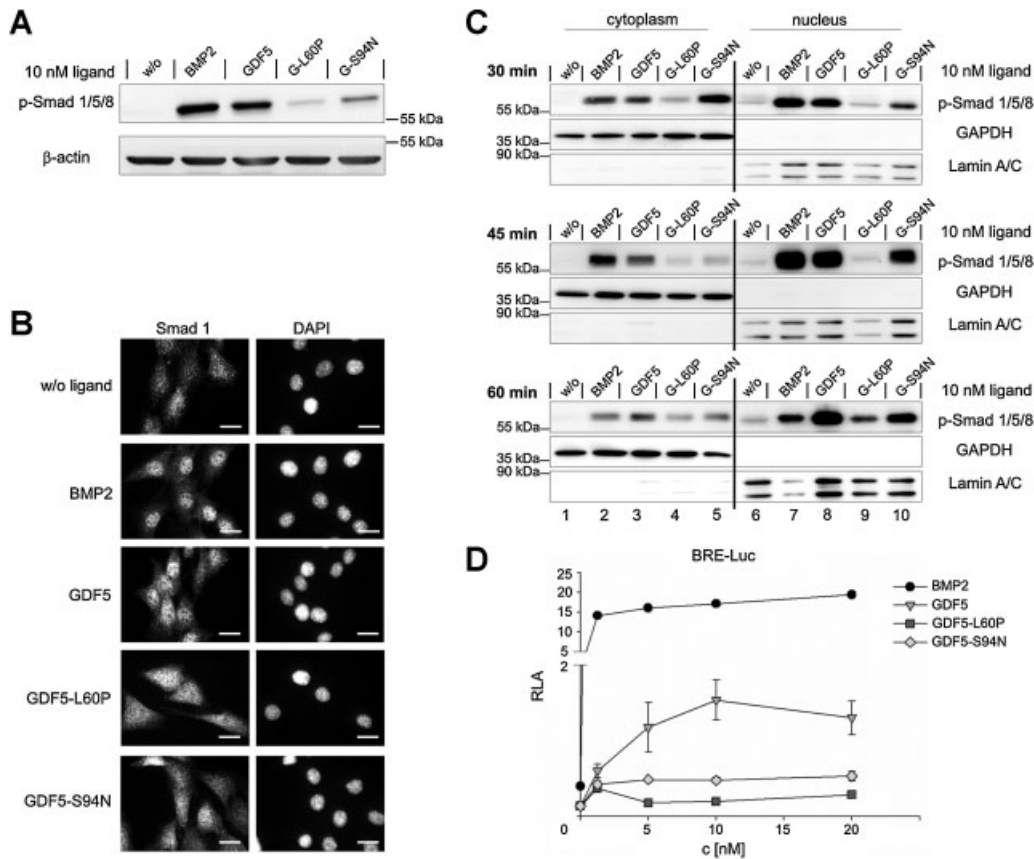


**Fig. 2.** GDF5-S94N and GDF5-L60P show decreased and delayed Smad signaling. (A) C2C12 cells were stimulated with BMP2, GDF5, GDF5-S94N (G-S94N), and GDF5-L60P (G-L60P) for 30 minutes and analyzed for Smad 1/5/8 phosphorylation.  $\beta$ -Actin serves as a loading control. (B) Immunofluorescent staining of Smad 1 nuclear translocation upon incubation for 30 minutes with indicated ligands. Nuclei were stained using DAPI. (C) C2C12 cells were exposed to BMP2, GDF5, GDF5-S94N (G-S94N) and GDF5-L60P (G-L60P) for the indicated times. After cell fractionation, the lysates were analyzed using a phospho-Smad 1/5/8 specific antibody. Anti-GAPDH and anti-Lamin A/C immunoblotting was used as control. (D) BRE-dependent reporter gene activity was examined in C2C12 cells after transfection with vectors encoding for the reporter genes and stimulation with BMP2, GDF5, GDF5-S94N, and GDF5-L60P. The results are shown as relative light activity (RLA) and represented as mean  $\pm$  SD of triplicate measurements in one out of three independent experiments.

toward an osteogenic cell fate by BMP or GDF stimulation,<sup>(43,44)</sup> they undergo myogenic differentiation upon serum deprivation.<sup>(45)</sup> These two processes counteract each other.<sup>(41,43)</sup> To investigate the effect of GDF5-S94N on C2C12 differentiation, we examined myogenesis by visualizing myotube formation. The myogenic marker protein myosin heavy chain (MyosinHC) was stained using a specific antibody. As expected, C2C12 cells underwent myogenic differentiation in ligand-free medium (Fig. 4A). However, a 5-day exposure to BMP2 and GDF5 prevented myogenic differentiation indicated by the lack of MyosinHC staining (Fig. 4A). Similar to the variant GDF5-L60P,<sup>(22)</sup> GDF5-S94N induced the formation of myotubes (Fig. 4A). These results were further confirmed by a luciferase reporter gene assay with a myogenin promoter (Fig. S1). We next performed qPCR investigating C2C12 differentiation by measuring mRNA levels of *myogenin* (*Myog*), a marker gene for myogenesis, as well as of *inhibitor of differentiation 1* (*Id1*) and *Runx2* (Fig. 4B–D). Analogous to the myotube formation experiment (Fig. 4A), both GDF5 mutants induced *Myog* mRNA comparable or even higher to nonstimulated cells 5 days after ligand treatment (Fig. 4B). The *Id* proteins prevent MyoD-dependent muscle-specific gene

transcription.<sup>(45)</sup> Expression of *Id1*<sup>(32)</sup> as well as *Runx2*,<sup>(46)</sup> the master gene of osteoblastic differentiation, are induced by activated Smads and responsible for osteogenic differentiation of C2C12 cells. In our studies, *Id1* and *Runx2* mRNA levels were moderately increased upon stimulation with BMP2 and GDF5, but were decreased upon exposure to either GDF5-S94N or GDF5-L60P compared with GDF5 (Fig. 4C, D).

To investigate chondrogenic differentiation driven by the key regulator GDF5 (7) or GDF5 mutants we analyzed the expression of chondrogenic marker genes by qPCR. As mRNA levels of *Sox9*, *Col2a1*, and *Opn* revealed, the chondrogenic character of ATDC5 cells was not affected by GDF5 mutants compared with GDF5 (Fig. 4E–G). Interestingly, mRNA level of *Runx2* (3.2-fold), *ALP* (10.4-fold), and *Col10a1* (16-fold), markers of mature or hypertrophic chondrocytes,<sup>(47–50)</sup> were upregulated upon stimulation with GDF5 (Fig. 4H–J) and much less upon GDF5-S94N and GDF5-L60P treatment (Fig. 4H–J). These results provide strong evidence for a reduced potential of GDF5 mutants to trigger chondrogenic maturation. Considering the altered binding affinities of mutants we conclude from this that proper GDF5 binding to both BMPRIA/IB and BMPRII is essential for the

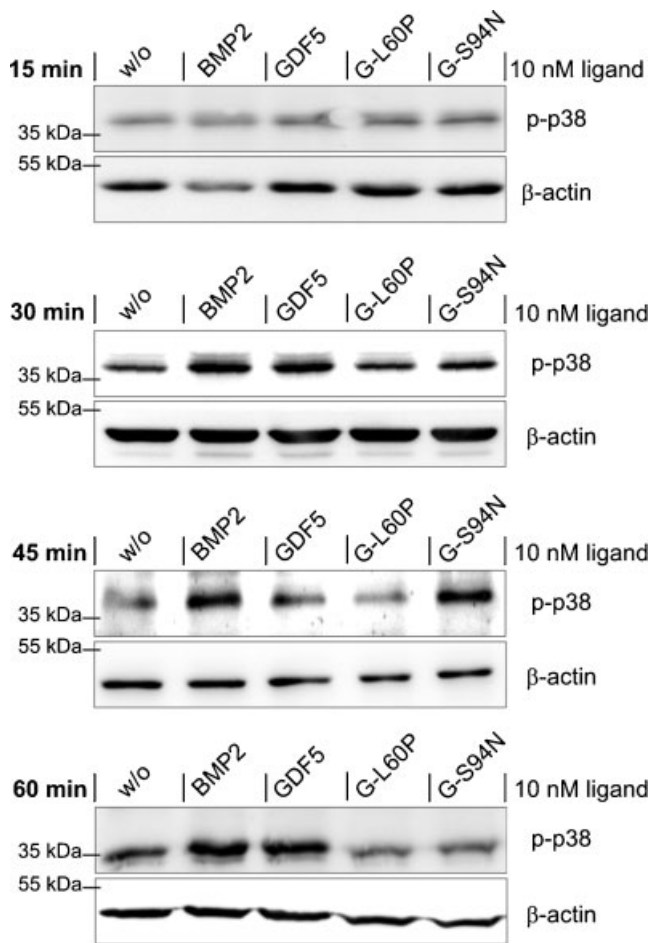


**Fig. 3.** GDF5-S94N induces delayed p38 MAPK signaling. C2C12 cells were treated with BMP2, GDF5, GDF5-S94N (G-S94N), and GDF5-L60P (G-L60P) for the indicated times and analyzed for p38 MAPK phosphorylation. Anti-β-actin immunoblotting was used as a loading control.

conversion of C2C12 myoblasts to osteoblast lineage, but more importantly for the chondrogenic maturation.

### GDF5-S94N potentially induces chondrogenesis in mouse micromass cultures

In the limb buds GDF5 is expressed throughout the phase of condensation of mesenchymal cells differentiating to chondrocytes and osteoblasts.<sup>(51)</sup> Therefore, we suggested that SYNS is a result of strongly enhanced GDF5 signaling. We found that GDF5-S94N, which is mutated within the knuckle epitope, can still activate the Smad 1/5/8 and the p38 MAPK pathway. However, the residual activity is not sufficient to promote chondrogenic differentiation. These data contradict the phenotype of SYNS as characterized by increased bone formation and joint fusion.

To clarify these results, we next examined the effect of GDF5-S94N on chondrogenic differentiation using mouse micromass cultures. The micromass culture model mimics the developmental process of endochondral ossification in vitro using isolated primary precursor cells and dense culture conditions. Pre-cartilage limb bud cells were seeded in high density and differentiated along a chondrocyte pathway when stimulated

with GDF5. The extracellular matrix (ECM) production can be detected using Alcian Blue staining.<sup>(34)</sup> We analyzed mouse micromass cultures exposed to GDF5 and GDF5 mutants for 6 days in a dose-response experiment. Surprisingly, treatment of micromass cultures with more than 0.1 nM GDF5-S94N caused significantly enhanced cartilaginous matrix production compared with GDF5 (Fig. 5A, B). As published recently, the variant GDF5-L60P showed only moderate chondrogenic differentiation<sup>(22)</sup> (Fig. 5A, B).

To gain further insights into the mechanism we analyzed the mRNA levels of different chondrogenic and osteogenic marker genes. Upon GDF5-L60P treatment the expression of the chondrogenic as well as osteogenic marker genes was reduced when compared with GDF5 (Fig. 5C–I). However, the transcription of the chondrogenic marker *Sox9*, *Col2a1*, and *Opn* were not affected by incubation with GDF5-S94N compared with GDF5 (Fig. 5C, D, S2A). *Col10a1* mRNA, expressed in chondrocytes, was reduced upon incubation with GDF5-S94N (Fig. 5E), reflecting the results in ATDC5 cells (Fig. 4E, F, G, J). Interestingly, in contrast to the ATDC5 cells, the expression of *Runx2*, *ALP* as well as the osteoblast-specific markers *Osterix* (*Sp7*) and *Ocn* were enhanced in GDF5-S94N-treated micromass cultures when compared with GDF5 (Fig. 5F–I). We excluded that this effect is caused by upregulation or missing inhibition of canonical Wnt signaling as it was observed in the BMPRIA conditional knock out mice.<sup>(52)</sup> *SOST*, *LRP5* (Fig. 5J, K), as well as *Dkk1* and *RANKL* (Fig. S2B, C), were not diminished by exposure to GDF5-S94N compared with GDF5.

Here we show for the first time, that despite defective BMPRII binding and early signaling defects, a mutation in the GDF5 knuckle epitope promotes chondrogenic differentiation and is responsible for the SYNS phenotype. Furthermore, our data suggest that the SYNS mutant GDF5-S94N affects other mechanisms than BMP receptor binding and canonical Wnt signaling leading to enhanced chondrogenesis.

### GDF5-S94N is resistant to noggin inhibition

BMP/GDF signaling is stringently regulated by extracellular modulator proteins, such as noggin and chordin (reviewed before).<sup>(17,53)</sup> SYNS was initially identified in patients with heterozygous *noggin* mutations.<sup>(4)</sup> In response to BMPs noggin is secreted in condensing cartilage and future joint spaces and prevents excessive exposure in a negative feedback loop.<sup>(16,22)</sup> The homodimeric antagonist interacts with both the wrist and the knuckle epitopes of BMP ligand members in a clamp-like fashion (Fig. 6A).<sup>(54)</sup> Hereby a large part of the convex wrist epitope is covered by the N-terminal clip domain (leucine 31 to serine 38) of the antagonist (Fig. 6A, B). Furthermore, the knuckle epitope of GDF5 is covered by the two pairs of β-strands forming finger 1 and 2 and the C-terminal half of the clip segment (leucine 43 to glutamic acid 48) of noggin (Fig. 6A, C). Thus, noggin blocks the interaction of BMPs/GDFs with both designated type I and type II receptors.<sup>(54)</sup>

The mutation S94N in GDF5 is located in the putative contact area with the C-terminal clip region of noggin (Fig. 6C). However, modeling of the interaction of this GDF5 variant with noggin suggests that the exchange of serine 94 to asparagine in GDF5

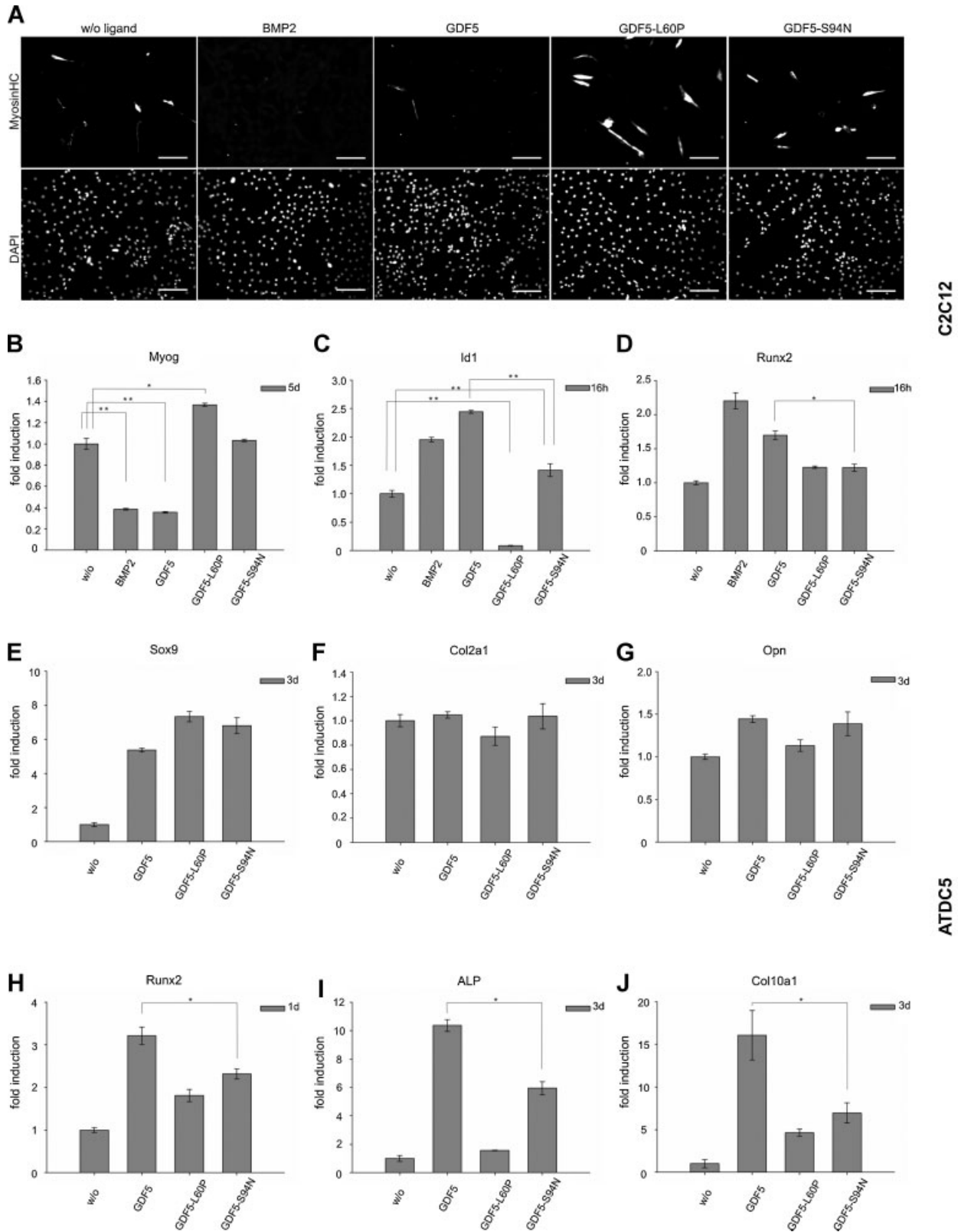


**Fig. 4.** GDF5-S94N and GDF5-L60P impair differentiation of C2C12 and ATDC5 cells. (A) C2C12 cells were incubated with BMP2, GDF5, GDF5-S94N, and GDF5-L60P for 5 days and analyzed for differentiation to myoblasts. Myosin heavy chain was stained using a specific antibody (above). Nuclei were stained using DAPI (below). (B–D) C2C12 cells were stimulated with indicated ligands and analyzed for expression of (B) myogenin mRNA, (C) Id1 mRNA, and (D) Runx2 mRNA by qPCR. (E–J) ATDC5 cells were incubated with 10 nM indicated ligands. Expression of Sox9 (E), Col2a1 (F), Osteopontin (Opn) (G), Runx2 (H), ALP (I), and Col10a1 (J) mRNA are depicted. Results are shown as means  $\pm$  SD of triplicate measurements in one out of two independent experiments (\* $p < 0.05$ ; \*\* $p < 0.005$ ;  $n = 3$ ).

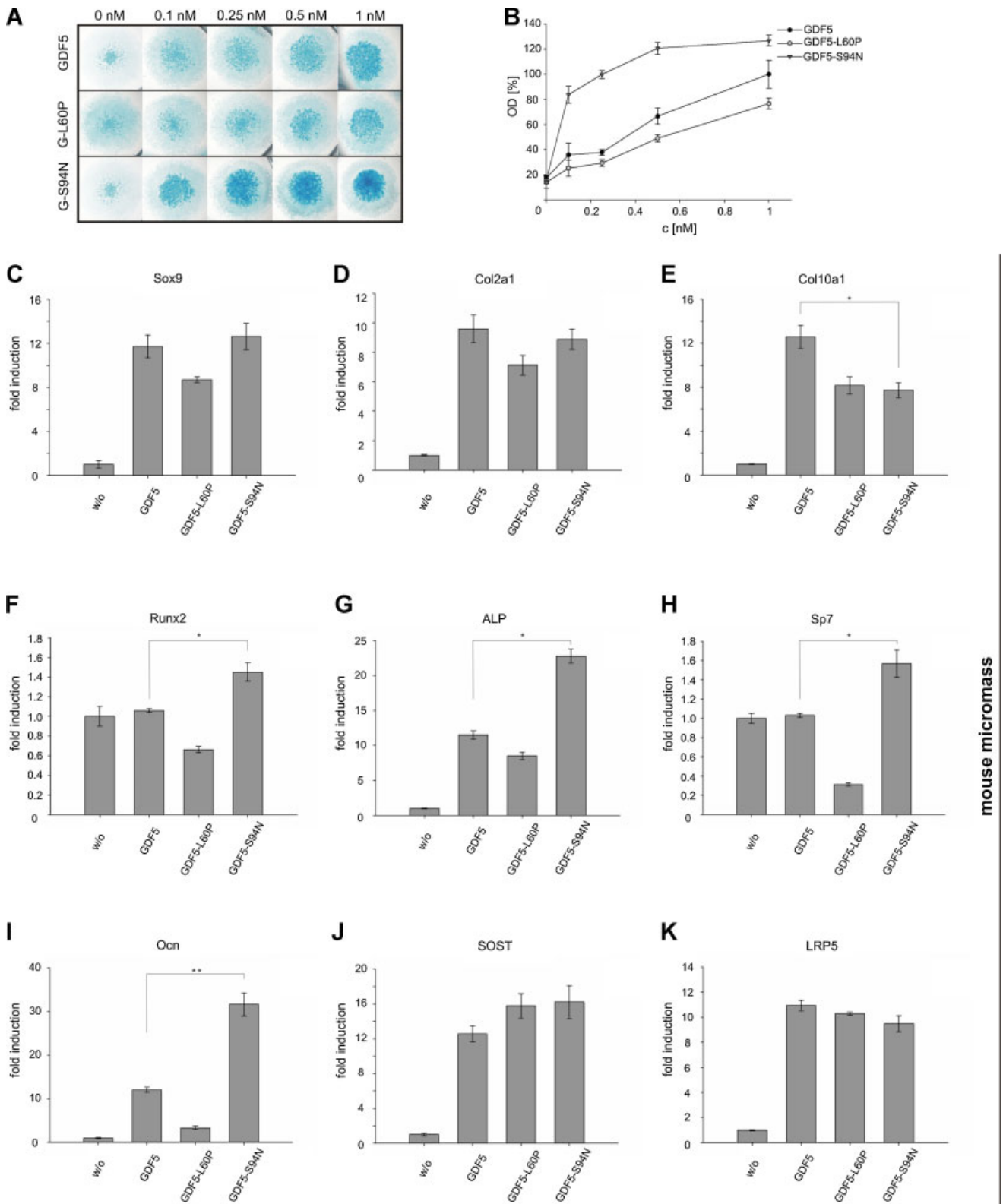


**Fig. 5.** GDF5 mutants affect the chondrogenic differentiation of mouse micromass cultures. (A) Mouse micromass cultures were incubated with increasing amounts of GDF5, GDF5-S94N (G-S94N), and GDF5-L60P (G-L60P) for 6 days and analyzed for cartilaginous matrix production by Alcian blue staining. Apoptosis of cells could be excluded (data not shown). (B) Optical density (OD) was quantified using BIO-1D and normalized to OD induced by 1 nM GDF5 (100%). (C–K) Expression of several chondrocytes and osteoblast marker genes in cultures treated with 1 nM ligand were detected by qPCR. Results are shown as means  $\pm$  SD of triplicate measurements of one biological sample ( $*p < 0.05$ ;  $**p < 0.005$ ;  $n = 3$ ).

would not impair the GDF5-noggin interaction because of steric hindrance. Despite this, SPR measurements revealed that GDF5-S94N binding to noggin ( $K_D \sim 3\text{--}4\text{ nM}$ ) was nevertheless fourfold decreased compared with GDF5 ( $K_D \sim 1\text{ nM}$ ) (Table 2). In contrast, the binding affinity of noggin to GDF5-L60P was not affected by the mutation in the wrist epitope of GDF5.<sup>(22)</sup>

To validate these *in vitro* results we exposed mouse prechondroblastic ATDC5 cells to GDF5-S94N and noggin and analyzed ALP expression, a marker gene expressed in both chondrocytes and osteoblasts (reviewed earlier).<sup>(55)</sup> An enzymatic ALP assay revealed that GDF5 and GDF5-S94N induced ALP activity (Fig. 6D). Corresponding to ALP mRNA level (Fig. 4I) ALP activity was slightly reduced in GDF5-S94N-treated cells. However, increasing amounts of noggin strongly inhibited the activity of GDF5, whereas variant GDF5-S94N was only minor affected (Fig. 6D). In consequence, when higher noggin concentrations were present, the increased signaling capacity of GDF5-S94N over GDF5 became obvious (Fig. 6D, 2.2-fold higher ALP activity compared with GDF5 in the presence of 50 nM noggin). This was even more pronounced by measuring the Smad-dependent reporter gene activity (Fig. 6E). Although in the absence of noggin GDF5-S94N showed less activity, the application of 5–20 nM noggin to either GDF5-S94N or GDF5 increased the signaling activity of GDF5-S94N over GDF5 by 1.5-fold to 3.6-fold, respectively (Fig. 6E).

To confirm these data we incubated mouse micromass cultures with 1 nM GDF5 or GDF5 mutants together with increasing concentrations of noggin. As expected, we observed strong antagonistic effects of noggin on the chondrogenesis induced by GDF5 (Fig. 6F, G). However, the cartilaginous matrix production induced by the variant GDF5-S94N was only marginally affected by noggin (Fig. 6F, G), although the endogenous noggin expression was even higher in those cells (Fig. 6H). In accordance with the SPR measurements, the weak chondrogenic activity of GDF5-L60P was antagonized by noggin already at low concentrations (0.25 nM noggin) (Fig. 6F, G).

To finally explain the different findings of GDF5 versus GDF5-S94N signaling capacity we investigated the endogenous expression of noggin in ATDC5 cells, C2C12 cells and micromass cultures. Figure 6I demonstrates that micromass cultures expressed  $10^6$ -fold more noggin compared with ATDC5 and C2C12 cells.

In summary we could show for the first time that serine 94 is a key residue in the GDF5 knuckle epitope, which interacts with the C-terminal clip region of noggin. The mutation GDF5-S94N causes resistance to ligand inhibition by noggin. Because the noggin-mediated negative feedback mechanism is impaired with GDF5-S94N, chondrogenic differentiation may not be limited in patients carrying this mutation. This observation is indeed reflected by the gain of function phenotype in SYNS.

## Discussion

Mutations in GDF5 are involved in a variety of genetic disorders, including chondrodysplasia, brachydactyly, SYM, and SYNS.<sup>(18,22,27,28)</sup> Most often these disorders are characterized by a frame shift mutation or an amino acid exchange located

within the type I receptor interaction site of GDF5, known as wrist epitope.<sup>(18,22)</sup> Previously described mutations in GDF5 and BMPRIB<sup>(1,2,56)</sup> suggest that signaling through BMPRIB is essential for chondrogenesis and osteogenesis, whereas GDF5-dependent signaling specifically through the low affinity receptor BMPRII has not been analyzed in detail.

This is the first study characterizing a GDF5 point mutation in the highly conserved knuckle epitope, which is the interaction site for BMPRII (Fig. 1). The mutation S94N in GDF5 was identified in patients suffering from SYNS.<sup>(26)</sup> Our study revealed that the variant GDF5-S94N exhibits a fivefold reduced binding affinity to BMPRII (Table 1). Because the phenotype indicates enhanced bone formation, we analyzed how a weaker binding of GDF5-S94N to BMPRII promotes rather than attenuates GDF5 signaling.

To gain further insights into the role of the knuckle epitope in GDF5 signaling, we compared GDF5-S94N not only to GDF5, but also to the variant GDF5-L60P,<sup>(22)</sup> which carries a point mutation close to the wrist epitope and is defective in type I receptor binding. The serine residue at position 94 is highly conserved within the BMP/GDF family (Fig. 1A) and homologous to serine 88 (S88) in BMP2. Interestingly, in the structures of the ternary complexes of BMP2 bound to BMPRIA and ActRII/IIIB two H-bonds exists between BMP2-S88 and ActRII/IIIB-L61 and BMP2-E109 and ActRII/IIIB-K37.<sup>(30,31)</sup> Direct structural data for the GDF5-BMPRII interaction are not yet available. However, according to our SPR measurements we suggest that the exchange of serine 94 to asparagine (S94N) in GDF5 affects H-bond formation to BMP type II receptors thereby causing a lower ligand binding affinity toward BMPRII and other type II receptors (ActRII and ActRIIB). *In vitro* this lower GDF5/BMPRII binding strength results in decreased and delayed Smad and non-Smad signaling and reduced transcriptional activity. These data therefore imply that despite of the lower BMPRII affinity, GDF5-S94N is still sufficient to induce BMPRI activation within the PFCs and/or recruitment of the type II receptor into the BISC. From this we speculate that ligand binding to BMPRII with a minimum affinity is required for the recruitment of cofactors, which are prerequisite for efficient signaling.<sup>(33,57)</sup>

The attenuated early Smad and non-Smad signaling contradicts the GDF5-S94N associated phenotype SYNS, characterized by enhanced chondrogenesis and osteogenesis through augmented GDF5 signaling. Therefore, we assumed that other pathways or cofactors might be involved promoting GDF5-induced signaling and chondrogenesis. Because GDF5 is required for limb mesenchymal cell condensation and enhanced chondrocyte hypertrophy and maturation,<sup>(58)</sup> we analyzed the effect of GDF5-S94N on mouse micromass cultures. These cells were directly obtained from limb buds.<sup>(34)</sup> When the endogenous expression levels of BMP receptors and antagonists shall be considered, micromass cultures more likely mimic the *in vivo* situation. In accordance with the SYNS phenotype, the mouse micromass assay revealed that GDF5-S94N accelerated chondrogenic matrix production compared with GDF5.

The first SYNS patients characterized, carried heterozygous mutations in the *noggin* gene.<sup>(4)</sup> Thus, we examined the binding affinity of the GDF5 mutants to noggin and the effects of noggin on GDF5 and GDF5 mutants in ATDC5 cells and in mouse micromass cultures. Our SPR measurements revealed that the

GDF5-S94N mutation reduces the affinity to noggin about fourfold compared with GDF5 (Table 2). Furthermore, in ATDC5 cells and in micromass cultures treated with increasing concentrations of noggin biological activity of GDF5-S94N was only marginally affected by noggin. This indicates that the amino

acid exchange of the highly conserved serine 94 to asparagine is sufficient to cause resistance to noggin inhibition. Most intriguingly, GDF5-S94N exceeded the GDF5 action only when noggin was present (Fig. 6). We observed this effect in ATDC5 and even stronger in micromass cultures by measuring ALP

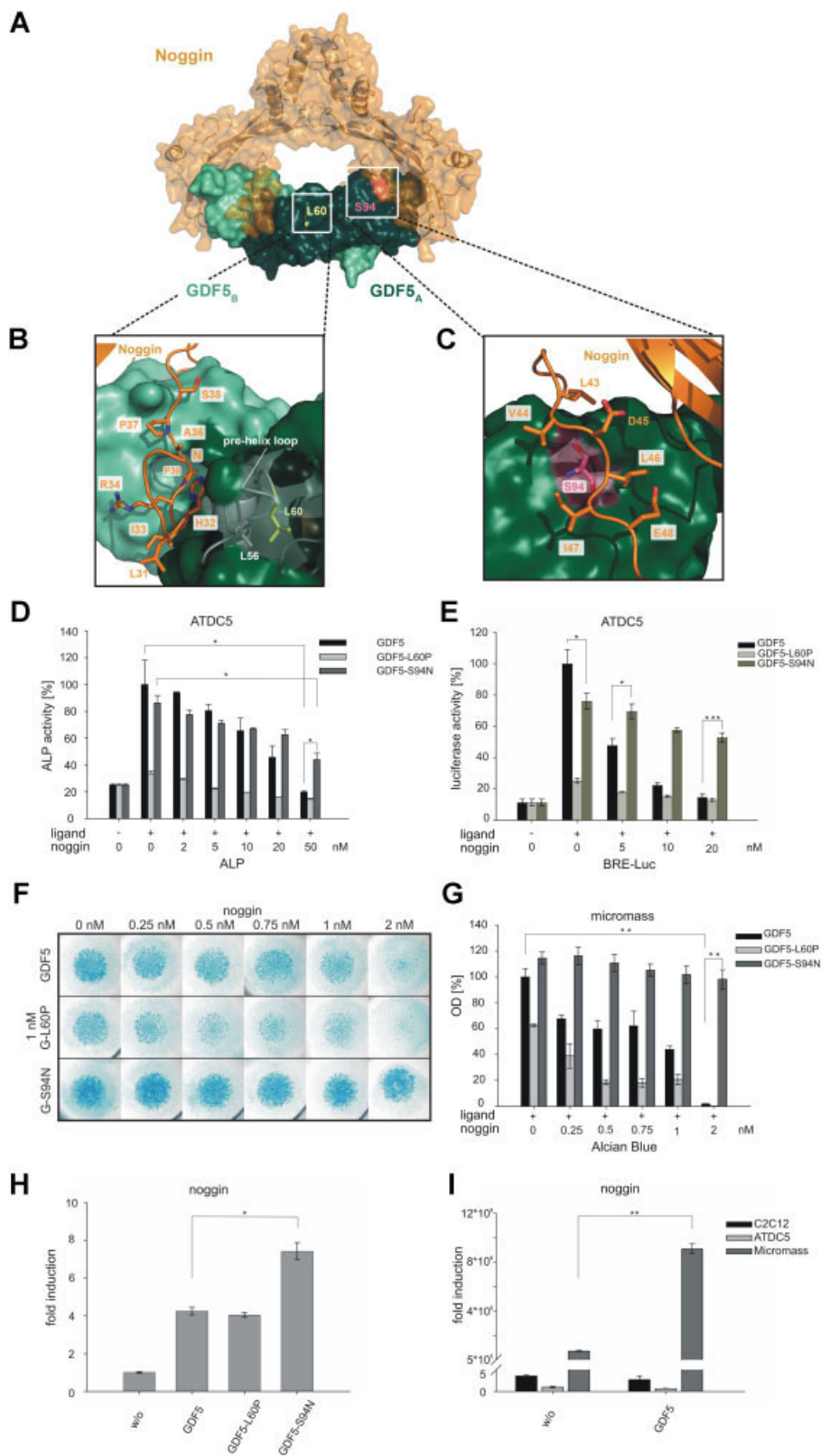


Fig. 6.

**Table 2.** Binding Affinities of GDF5 Mutants to Immobilized Noggin (SPR Measurement)

Ligand	$K_D$ (nM)		Ref.
	noggin		
BMP2	1.9		
GDF5	0.97		
GDF5-L60P	1.5		(22)
GDF5-S94N	3.6		

Mean values from two experiments using at least six different analyte concentrations.

activity (Fig. 6D; 2.2-fold higher activity of GDF5-S94N over GDF5 in the presence of 50 nM noggin), Smad-dependent reporter gene activity (Fig. 6E; 3.6-fold higher activity of GDF5-S94N over GDF5 in the presence of 20 nM noggin), and ECM production (Fig. 6F, G; 52-fold higher activity of GDF5-S94N over GDF5 in the presence of 2 nM noggin).

The reduced signaling observed in C2C12 and ATDC5 cells in the absence of recombinant noggin was not affected by endogenous noggin, because it was not expressed (Fig. 6I). Interestingly, in mouse micromass noggin expression was induced by both GDF5 and even stronger by GDF5-S94N (Fig. 6H). This negative feedback mechanism is converted to a feedforward situation in the mutant.

Resistance to noggin inhibition caused by a mutation within the knuckle epitope of GDF5 has not been described so far. Several mutations in the fingers 1 and 2 of noggin result in SYM and carpal/tarsal fusions;<sup>(3–6)</sup> these data already indicated that the interaction between noggin and the knuckle epitope of GDF5 is crucial for bone and joint formation. However, the dynamics of the noggin–BMP/GDF interaction are not well understood. Looking at the structural features of noggin including the flexible N-terminal clip, we propose that small alterations in the interaction between GDF5 and the C-terminal half of noggin's clip segment results in resistance to noggin inhibition. Furthermore, it might be that the BMP/GDF5–noggin interaction is also affected by other cofactors.

GDF5-N64K/T (N445K/T when the proprotein numbering is considered) was also described as a mutant resistant to noggin inhibition causing SYNS.<sup>(27)</sup> In contrast to GDF5-S94N, the exchange of asparagine 64 to lysine/threonine (N64K/T) is

located outside the wrist epitope of GDF5<sup>(37)</sup> and showed no changes in binding affinity to BMPRIA/IB<sup>(27)</sup> or noggin when compared with GDF5. However, GDF5-N64T induced a higher ALP activity in C2C12 cells and an enhanced cartilage production in micromass cultures, even in the presence of noggin.<sup>(22)</sup> Lysine 64 (K64) of GDF5 is conserved also in BMP9 and BMP10; both are insensitive to noggin.<sup>(27)</sup> Moreover, lysine 60 (K60) in BMP6 has been described as a key residue for BMP6'-specific resistance to noggin inhibition.<sup>(59)</sup> Surprisingly, the identified key residues for noggin resistance GDF5-K64 or BMP6-K60 do not directly interact with noggin.<sup>(54,60)</sup> From this we conclude that the mechanism by which noggin antagonizes BMP and GDF5 ligands is yet not fully understood and might include other determinants or indirect mechanism as we proposed for GDF5-L60P.

Leucine 60 (L60) is almost completely buried in the core of GDF5 but has hydrophobic contacts with residue L56 in the prehelix loop of GDF5 (Fig. 6B). Therefore, the mutation GDF5-L60P might result in a conformational change of the prehelix loop, which in turn affects and destroys the interaction with BMPRIA.<sup>(35)</sup> The missing interaction of GDF5-L60P with BMPRIA/IB resulted in a lack of Smad signaling and/or p38 MAPK activation (Figs. 2, 3), which are important for cartilage formation.<sup>(13,14,61)</sup> This was reflected in micromass cultures. Less than 1 nM GDF5-L60P caused a reduced ECM production and expression of chondrocyte and osteoblast marker (Fig. 5A, B, F–J). However, incubation of micromass cultures with more than 1 nM GDF5-L60P showed a slight induction of cartilage production. This can be traced back to the higher expression of BMPRIA in limb bud cells,<sup>(56)</sup> which rescues the missing interaction with BMPRIA. The same effect could be observed in C2C12 cells overexpressing BMPRIA; here GDF5-L60P induced both BRE-dependent reporter gene and ALP activity (Fig. S3).

Signaling induced by GDF5-L60P appeared to be more sensitive toward noggin inhibition in micromass cultures, whereas SPR measurements demonstrated that the binding affinity to noggin was not altered for GDF5-L60P.<sup>(22)</sup> However, we cannot exclude that the mutation GDF5-L60P might result in a conformational change of the prehelix loop making the wrist epitope more accessible to proline 35 (P35) within the N-terminal noggin clip region. This facilitates the hydrophobic knob-into-hole interaction in the center of the wrist epitope (Fig. 6B).<sup>(35)</sup> Therefore, the temporal and spatial expression of GDF5-L60P, BMPRIA, and noggin regulates the development of the phalanges and results in BDA2 characterized by missing middle

**Fig. 6.** GDF5-S94N mutant is resistant to noggin inhibition. (A) A homology model of the GDF5–noggin complex. The GDF5<sub>AB</sub> dimer is shown in light and dark green, the noggin clamp is indicated in ochre. GDF5 mutations are indicated: GDF5-S94N (pink) and GDF5-L60P (yellow). (B) Surface of the GDF5 wrist epitope and the N-terminal noggin clip. Ligand-interacting residues of noggin are indicated in orange. L56 (gray) and L60 (yellow) of GDF5 are labeled. (C) Zoom into the GDF5 knuckle epitope (green) and the C-terminal part of the noggin clip (orange). Ligand-interacting residues of noggin are shown in orange. GDF5-S94N is depicted in pink. (D) ATDC5 cells were incubated with 5 nM GDF5, GDF5-S94N, or GDF5-L60P and with increasing amounts of noggin. ALP activity was normalized to ALP activity induced by 5 nM GDF5 (100%). The results are depicted as means  $\pm$  SD of triplicate measurements and represent one out of three independent experiments. (E) ATDC5 cells were used for BRE-Luc reporter gene assay and incubated with 5 nM wtGDF5, GDF5-S94N, or GDF5-L60P and with increasing amounts of noggin. The relative luciferase activity was normalized to the relative luciferase activity induced by 5 nM wtGDF5 (100%). It is depicted as means  $\pm$  SD of triplicate measurements and represents one out of two independent experiments. (F) Mouse micromass cells were incubated with 1 nM GDF5, GDF5-S94N (G-S94N), and GDF5-L60P (G-L60P) and increasing concentrations of noggin. Cartilaginous production was detected after Alcian Blue staining. (G) OD was normalized to OD induced by 1 nM GDF5 (100%). (H) Mouse micromass cells were stimulated with indicated ligands for 6 days and analyzed for expression of noggin mRNA by qPCR. Results are shown as mean  $\pm$  SD of triplicate measurements of one biological sample. (I) Expression of noggin mRNA in C2C12 cells, ATDC5 cells, and micromass cultures are compared. mRNA levels are normalized to unstimulated ATDC5 cells (\* $p$  < 0.02; \*\* $p$  < 0.002; \*\*\* $p$  < 0.0002;  $n$  = 3).

phalanges in finger II and hypoplasia of the middle phalanges in finger V.<sup>(22)</sup>

Taken together, we have identified serine 94 (S94) as a specific residue within the GDF5 knuckle epitope, which is important for rapid signal propagation and interaction with the C-terminal part of the clip region of noggin. The mutation S94N results in lower affinity to BMPRII. GDF5-S94N therefore shows reduced signaling via the Smad pathway and non-Smad pathways, both important for chondrogenesis. Furthermore, the mutation S94N results in a lower affinity of the mutant to noggin and prevents the inhibition by noggin in a negative feedback loop as it is observed for GDF5. Consequently, the simultaneous expression of GDF5-S94N and noggin in limb buds allows that the residual activity of GDF5-S94N potently induces chondrogenesis, which is not counterbalanced by noggin. This accounts for accelerated endochondral ossification as it becomes visible in patients suffering from SYNS (Fig. 7). In the study presented here we uncovered the molecular mechanism by which GDF5-S94N

mutation causes SYNS. We highlight the potential of GDF5 knuckle epitope mutants to be attractive candidates for therapeutical applications in the field of regenerative medicine.

## Disclosures

All the authors state that they have no conflict of interests.

## Acknowledgments

We thank C. Sieber and C. Krause for critical reading of the manuscript. We thank J. Kopf for technical support and R. Zavala for the reporter construct Myg-Luc. This work has been supported by Deutsche Forschungsgemeinschaft (DFG) SFB 760 PK and by the Berlin Brandenburg School for Regenerative Therapies (BSRT) Graduate School 203 for providing C.H. with a fellowship.

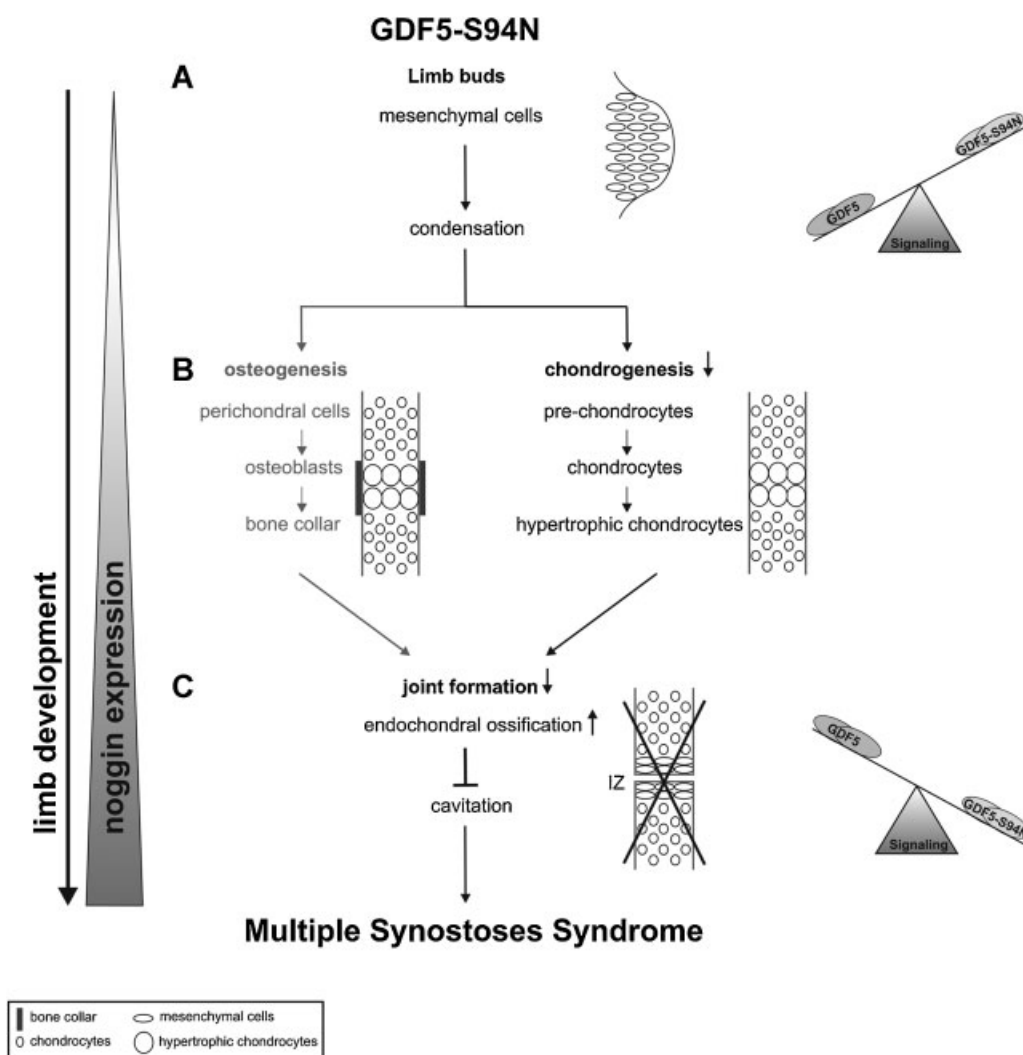


**Fig. 7.** Noggin-resistance of GDF5-S94N during limb development results in the Multiple Synostoses Syndrome. (A) In limb buds GDF5-S94N induces the condensation of mesenchymal cells, which, as a consequence of the mutation, leads to (B) reduced generation of chondrocytes. Due to the reduced signaling capacity GDF5-S94N impairs chondrogenesis. (C) In future joint spaces, chondrocytes secrete GDF5-S94N as well as noggin to form the interzone (IZ). GDF5-S94N is resistant to noggin inhibition. When noggin expression increases during promotion of limb development (left), the signaling activities of GDF5-S94N overrides the action of GDF5 (right side). This results in enhanced endochondral ossification and missing cavitation. As a consequence of this noggin-resistance GDF5-S94N accumulates a gain of function, which is reflected in the Multiple Synostoses Syndrome.

Author's roles: Study design: PK; Study conduct: GKS, CH, HS, TM; Data collection and analysis: GKS, CH, HS, JN, PK; Data interpretation: GKS, TM, PK; Contributed reagents/materials: WS, FP; Drafting manuscript: GKS, CH, PK; Approving final version of manuscript: GKS, CH, HS, JN, FP, WS, TM, PK.

## References

1. Lehmann K, Seemann P, Stricker S, Sammar M, Meyer B, Suring K, Majewski F, Tinschert S, Grzeschik KH, Muller D, Knaus P, Nurnberg P, Mundlos S. Mutations in bone morphogenetic protein receptor 1B cause brachydactyly type A2. *Proc Natl Acad Sci USA*. 2003;100:12277–82.
2. Lehmann K, Seemann P, Boergemann J, Morin G, Reif S, Knaus P, Mundlos S. A novel R486Q mutation in BMPRI1B resulting in either a brachydactyly type C/symphalangism-like phenotype or brachydactyly type A2. *Eur J Hum Genet*. 2006;14:1248–54.
3. Lehmann K, Seemann P, Silan F, Goecke TO, Irgang S, Kjaer KW, Kjaergaard S, Mahoney MJ, Morlot S, Reissner C, Kerr B, Wilkie AO, Mundlos S. A new subtype of brachydactyly type B caused by point mutations in the bone morphogenetic protein antagonist NOGGIN. *Am J Hum Genet*. 2007;81:388–96.
4. Gong Y, Krakow D, Marcelino J, Wilkin D, Chitayat D, Babul-Hirji R, Hudgins L, Cremers CW, Cremers FP, Brunner HG, Reinker K, Rimoin DL, Cohn DH, Goodman FR, Reardon W, Patton M, Francomano CA, Warman ML. Heterozygous mutations in the gene encoding noggin affect human joint morphogenesis. *Nat Genet*. 1999;21:302–4.
5. Dixon ME, Armstrong P, Stevens DB, Bamshad M. Identical mutations in NOG can cause either tarsal/carpal coalition syndrome or proximal symphalangism. *Genet Med*. 2001;3:349–53.
6. Takahashi T, Takahashi I, Komatsu M, Sawaiishi Y, Higashi K, Nishimura G, Saito H, Takada G. Mutations of the NOG gene in individuals with proximal symphalangism and multiple synostosis syndrome. *Clin Genet*. 2001;60:447–51.
7. Storm EE, Huynh TV, Copeland NG, Jenkins NA, Kingsley DM, Lee SJ. Limb alterations in brachypodism mice due to mutations in a new member of the TGF beta-superfamily. *Nature*. 1994;368:639–43.
8. Pacifici M, Koyama E, Iwamoto M. Mechanisms of synovial joint and articular cartilage formation: recent advances, but many lingering mysteries. *Birth Defects Res C Embryo Today*. 2005;75:237–48.
9. Sieber C, Ploger F, Schwappacher R, Bechtold R, Hanke M, Kawai S, Muraki Y, Katsuura M, Kimura M, Rechtman MM, Henis YI, Pohl J, Knaus P. Monomeric and dimeric GDF-5 show equal type I receptor binding and oligomerization capability and have the same biological activity. *Biol Chem*. 2006;387:451–60.
10. Heinecke K, Seher A, Schmitz W, Mueller TD, Sebald W, Nickel J. Receptor oligomerization and beyond: a case study in bone morphogenetic proteins. *BMC Biol*. 2009;7:59.
11. Nohe A, Hassel S, Ehrlich M, Neubauer F, Sebald W, Henis YI, Knaus P. The mode of bone morphogenetic protein (BMP) receptor oligomerization determines different BMP-2 signaling pathways. *J Biol Chem*. 2002;277:5330–8.
12. Hartung A, Bitton-Worms K, Rechtman MM, Wenzel V, Boergemann JH, Hassel S, Henis YI, Knaus P. Different routes of bone morphogenetic protein (BMP) receptor endocytosis influence BMP signaling. *Mol Cell Biol*. 2006;26:7791–805.
13. Nakamura K, Shirai T, Morishita S, Uchida S, Saeki-Miura K, Makishima F. p38 mitogen-activated protein kinase functionally contributes to chondrogenesis induced by growth/differentiation factor-5 in ATDC5 cells. *Exp Cell Res*. 1999;250:351–63.
14. Retting KN, Song B, Yoon BS, Lyons KM. BMP canonical Smad signaling through Smad1 and Smad5 is required for endochondral bone formation. *Development*. 2009;136:1093–104.
15. Yoon BS, Lyons KM. Multiple functions of BMPs in chondrogenesis. *J Cell Biochem*. 2004;93:93–103.
16. Brunet LJ, McMahon JA, McMahon AP, Harland RM. Noggin, cartilage morphogenesis, and joint formation in the mammalian skeleton. *Science*. 1998;280:1455–7.
17. Krause C, Guzman A, Knaus P. Noggin. *Int J Biochem Cell Biol*. 2011;43:478–81.
18. Thomas JT, Lin K, Nandedkar M, Camargo M, Cervenka J, Luyten FP. A human chondrodysplasia due to a mutation in a TGF-beta superfamily member. *Nat Genet*. 1996;12:315–7.
19. Szczaluba K, Hilbert K, Obersztyn E, Zabel B, Mazurczak T, Kozłowski K, Du Pan syndrome phenotype caused by heterozygous pathogenic mutations in CDMP1 gene. *Am J Med Genet A*. 2005;138:379–83.
20. Faiyaz-UI-Haque M, Faqeih EA, Al-Zaidan H, Al-Shammary A, Zaidi SH. Grebe-type chondrodysplasia: a novel missense mutation in a conserved cysteine of the growth differentiation factor 5. *J Bone Miner Metab*. 2008;26:648–52.
21. Everman DB, Bartels CF, Yang Y, Yanamandra N, Goodman FR, Mendoza-Londono JR, Savarirayan R, White SM, Graham JM Jr, Gale RP, Svarch E, Newman WG, Kleckers AR, Francomano CA, Govindaiah V, Singh L, Morrison S, Thomas JT, Warman ML. The mutational spectrum of brachydactyly type C. *Am J Med Genet*. 2002;112:291–6.
22. Seemann P, Schwappacher R, Kjaer KW, Krakow D, Lehmann K, Dawson K, Stricker S, Pohl J, Ploger F, Staub E, Nickel J, Sebald W, Knaus P, Mundlos S. Activating and deactivating mutations in the receptor interaction site of GDF5 cause symphalangism or brachydactyly type A2. *J Clin Invest*. 2005;115:2373–81.
23. Ploger F, Seemann P, Schmidt-von Kegler M, Lehmann K, Seidel J, Kjaer KW, Pohl J, Mundlos S. Brachydactyly type A2 associated with a defect in proGDF5 processing. *Hum Mol Genet*. 2008;17:1222–33.
24. Wang X, Xiao F, Yang Q, Liang B, Tang Z, Jiang L, Zhu Q, Chang W, Jiang J, Jiang C, Ren X, Liu JY, Wang QK, Liu M. A novel mutation in GDF5 causes autosomal dominant symphalangism in two Chinese families. *Am J Med Genet A*. 2006;140A:1846–53.
25. Yang W, Cao L, Liu W, Jiang L, Sun M, Zhang D, Wang S, Lo WH, Luo Y, Zhang X. Novel point mutations in GDF5 associated with two distinct limb malformations in Chinese: brachydactyly type C and proximal symphalangism. *J Hum Genet*. 2008;53:368–74.
26. Akarsu A, Rezale T, Demirtas M, Farhud DD, Sarfarazi M. Multiple synostosis type 2 (SYNS2) maps to 20q11.2 and caused by a missense mutation in the growth/differentiation factor 5 (GDF5). *Am J Hum Genet Suppl*. 1999;65A:281.
27. Seemann P, Brehm A, König J, Reissner C, Stricker S, Kuss P, Haupt J, Renninger S, Nickel J, Sebald W, Groppe JC, Ploger F, Pohl J, Schmidt-von Kegler M, Walther M, Gassner I, Rusu C, Janecke AR, Dathe K, Mundlos S. Mutations in GDF5 reveal a key residue mediating BMP inhibition by NOGGIN. *PLoS Genet*. 2009;5:e1000747.
28. Dawson K, Seeman P, Sebald E, King L, Edwards M, Williams J 3rd, Mundlos S, Krakow D. GDF5 is a second locus for multiple-synostosis syndrome. *Am J Hum Genet*. 2006;78:708–12.
29. Kirsch T, Nickel J, Sebald W. BMP-2 antagonists emerge from alterations in the low-affinity binding epitope for receptor BMPRII. *EMBO J*. 2000;19:3314–24.
30. Allendorph GP, Vale WW, Choe S. Structure of the ternary signaling complex of a TGF-beta superfamily member. *Proc Natl Acad Sci USA*. 2006;103:7643–8.
31. Weber D, Kotszsch A, Nickel J, Harth S, Seher A, Mueller U, Sebald W, Mueller TD. A silent H-bond can be mutationally activated for high-affinity interaction of BMP-2 and activin type IIB receptor. *BMC Struct Biol*. 2007;7:6.
32. Korchynskiy O, ten Dijke P. Identification and functional characterization of distinct critically important bone morphogenetic protein-

- specific response elements in the Id1 promoter. *J Biol Chem.* 2002; 277:4883–91.
33. Schwappacher R, Weiske J, Heining E, Ezerski V, Marom B, Henis YI, Huber O, Knaus P. Novel crosstalk to BMP signalling: cGMP-dependent kinase I modulates BMP receptor and Smad activity. *EMBO J.* 2009;28:1537–50.
  34. Karamboulas K, Dranse HJ, Underhill TM. Regulation of BMP-dependent chondrogenesis in early limb mesenchyme by TGFbeta signals. *J Cell Sci.* 2010;123:2068–76.
  35. Kotsch A, Nickel J, Seher A, Sebald W, Muller TD. Crystal structure analysis reveals a spring-loaded latch as molecular mechanism for GDF-5-type I receptor specificity. *EMBO J.* 2009;28:937–47.
  36. Greenwald J, Groppa J, Gray P, Wiater E, Kwiatkowski W, Vale W, Choe S. The BMP7/ActRII extracellular domain complex provides new insights into the cooperative nature of receptor assembly. *Mol Cell.* 2003;11:605–17.
  37. Nickel J, Kotsch A, Sebald W, Mueller TD. A single residue of GDF-5 defines binding specificity to BMP receptor IB. *J Mol Biol.* 2005;349: 933–47.
  38. Kirsch T, Sebald W, Dreyer MK. Crystal structure of the BMP-2-BRIA ectodomain complex. *Nat Struct Biol.* 2000;7:492–6.
  39. Gilboa L, Nohe A, Geissendorfer T, Sebald W, Henis YI, Knaus P. Bone morphogenetic protein receptor complexes on the surface of live cells: a new oligomerization mode for serine/threonine kinases. *Mol Biol Cell.* 2000;11:1023–35.
  40. Hassel S, Schmitt S, Hartung A, Roth M, Nohe A, Petersen N, Ehrlich M, Henis YI, Sebald W, Knaus P. Initiation of Smad-dependent and Smad-independent signaling via distinct BMP-receptor complexes. *J Bone Joint Surg Am.* 2003;85-A (Suppl 3): 44–51.
  41. Nojima J, Kanomata K, Takada Y, Fukuda T, Kokabu S, Ohte S, Takada T, Tsukui T, Yamamoto TS, Sasanuma H, Yoneyama K, Ueno N, Okazaki Y, Kamijo R, Yoda T, Katagiri T. Dual roles of smad proteins in the conversion from myoblasts to osteoblastic cells by bone morphogenetic proteins. *J Biol Chem.* 2010;285:15577–86.
  42. Gallea S, Lallemand F, Atfi A, Rawadi G, Ramez V, Spinella-Jaegle S, Kawai S, Faucheu C, Huet L, Baron R, Roman-Roman S. Activation of mitogen-activated protein kinase cascades is involved in regulation of bone morphogenetic protein-2-induced osteoblast differentiation in pluripotent C2C12 cells. *Bone.* 2001;28:491–8.
  43. Katagiri T, Yamaguchi A, Komaki M, Abe E, Takahashi N, Ikeda T, Rosen V, Wozney JM, Fujisawa-Sehara A, Suda T. Bone morphogenetic protein-2 converts the differentiation pathway of C2C12 myoblasts into the osteoblast lineage. *J Cell Biol.* 1994;127:1755–66.
  44. Aoki H, Fujii M, Imamura T, Yagi K, Takehara K, Kato M, Miyazono K. Synergistic effects of different bone morphogenetic protein type I receptors on alkaline phosphatase induction. *J Cell Sci.* 2001;114: 1483–9.
  45. Benezra R, Davis RL, Lockshon D, Turner DL, Weintraub H. The protein Id: a negative regulator of helix-loop-helix DNA binding proteins. *Cell.* 1990;61:49–59.
  46. Lee KS, Hong SH, Bae SC. Both the Smad and p38 MAPK pathways play a crucial role in Runx2 expression after induction by transforming growth factor-beta and bone morphogenetic protein. *Oncogene.* 2002;21:7156–63.
  47. Inada M, Yasui T, Nomura S, Miyake S, Deguchi K, Himeno M, Sato M, Yamagiwa H, Kimura T, Yasui N, Ochi T, Endo N, Kitamura Y, Kishimoto T, Komori T. Maturational disturbance of chondrocytes in Cbfa1-deficient mice. *Dev Dyn.* 1999;214:279–90.
  48. Kim IS, Otto F, Zabel B, Mundlos S. Regulation of chondrocyte differentiation by Cbfa1. *Mech Dev.* 1999;80:159–70.
  49. Schmid TM, Linsenmayer TF. Developmental acquisition of type X collagen in the embryonic chick tibiotarsus. *Dev Biol.* 1985;107: 373–81.
  50. Roach HI. Association of matrix acid and alkaline phosphatases with mineralization of cartilage and endochondral bone. *Histochem J.* 1999;31:53–61.
  51. Francis-West PH, Abdelfattah A, Chen P, Allen C, Parish J, Ladher R, Allen S, MacPherson S, Luyten FP, Archer CW. Mechanisms of GDF-5 action during skeletal development. *Development.* 1999;126: 1305–15.
  52. Kamiya N, Ye L, Kobayashi T, Mochida Y, Yamauchi M, Kronenberg HM, Feng JQ, Mishina Y. BMP signaling negatively regulates bone mass through sclerostin by inhibiting the canonical Wnt pathway. *Development.* 2008;135:3801–11.
  53. Rider CC, Mulloy B. Bone morphogenetic protein and growth differentiation factor cytokine families and their protein antagonists. *Biochem J.* 2010;429:1–12.
  54. Groppa J, Greenwald J, Wiater E, Rodriguez-Leon J, Economides AN, Kwiatkowski W, Affolter M, Vale WW, Belmonte JC, Choe S. Structural basis of BMP signalling inhibition by the cystine knot protein Noggin. *Nature.* 2002;420:636–42.
  55. Shum L, Coleman CM, Hatakeyama Y, Tuan RS. Morphogenesis and dysmorphogenesis of the appendicular skeleton. *Birth Defects Res C Embryo Today.* 2003;69:102–22.
  56. Yi SE, Daluiski A, Pederson R, Rosen V, Lyons KM. The type I BMP receptor BMPRII is required for chondrogenesis in the mouse limb. *Development.* 2000;127:621–30.
  57. Chan MC, Nguyen PH, Davis BN, Ohoka N, Hayashi H, Du K, Lagna G, Hata A. A novel regulatory mechanism of the bone morphogenetic protein (BMP) signaling pathway involving the carboxyl-terminal tail domain of BMP type II receptor. *Mol Cell Biol.* 2007;27: 5776–89.
  58. Coleman CM, Tuan RS. Growth/differentiation factor 5 enhances chondrocyte maturation. *Dev Dyn.* 2003;228:208–16.
  59. Song K, Krause C, Shi S, Patterson M, Suto R, Grgurevic L, Vukicevic S, van Dinther M, Falb D, Ten Dijke P, Alaoui-Ismaïli MH. Identification of a key residue mediating bone morphogenetic protein (BMP)-6 resistance to noggin inhibition allows for engineered BMPs with superior agonist activity. *J Biol Chem.* 2010;285:12169–80.
  60. Kotsch A, Nickel J, Seher A, Heinecke K, van Geersdaele L, Herrmann T, Sebald W, Mueller TD. Structure analysis of bone morphogenetic protein-2 type I receptor complexes reveals a mechanism of receptor inactivation in juvenile polyposis syndrome. *J Biol Chem.* 2008;283: 5876–87.
  61. Greenblatt MB, Shim JH, Zou W, Sitara D, Schweitzer M, Hu D, Lotinun S, Sano Y, Baron R, Park JM, Arthur S, Xie M, Schneider MD, Zhai B, Gygi S, Davis R, Glimcher LH. The p38 MAPK pathway is essential for skeletogenesis and bone homeostasis in mice. *J Clin Invest.* 2010;120:2457–73.
  62. Keller S, Nickel J, Zhang JL, Sebald W, Mueller TD. Molecular recognition of BMP-2 and BMP receptor IA. *Nat Struct Mol Biol.* 2004; 11:481–8.